Advances in Nano Research, *Vol. 18, No. 4 (2025) 307-319*
https://doi.org/10.12989/anr.2025.18.4.307

Investigating nonlinear dynamics and vibration of composite cylindrical shells with Graphene-origami enabled cores

Farzad Ebrahimi* and Seyede Zahra Mirsadoghi

Department of Mechanical Engineering, Faculty of Engineering, Imam Khomeini International University, Qazvin, Iran

(*Received December 17, 2020, Revised February 16, 2025, Accepted February 20, 2025*)

Abstract. This work investigates the nonlinear dynamic response and oscillation analysis of composite-structured cylindrical shells. The core of this structure is constructed from graphene origami (Gori), a metamaterial with a negative Poisson's ratio (NPR). The exterior sides of this structure are composed of aluminum. To precisely determine the dynamic response of a framework, it is subjected to specific conditions, including external excitation and pre-loading. The governing Equations for the behavior and motion of the cylindrical shell are obtained utilizing the enhanced Donnell theory and the nonlinear von Karman theory, facilitating a more precise description of the shell's nonlinear behavior. This study has addressed the boundary conditions for the cylindrical shell in a straight forward manner. The governing Equations of the structure have been resolved utilizing the Galerkin's approach, and the resultant numerical results have been analyzed. This article aims to examine the linear and nonlinear vibration response ratios of cylindrical shells, taking into account the effect of negative Poisson's ratio and its nonlinear dynamic analysis. The findings of the current investigation are shown in the relevant tables alongside related research. This research examines the impact of oscillations in the geometric parameters of the structure and the characteristics of graphene origami as critical variables. The results are illustrated in figures, and their impact on the dynamic and vibrational characteristics of the structure is examined. This research investigates the dynamic behavior of cylindrical composite shells and offers solutions to the issues within this domain by analyzing the applications of this construction.
Keywords: auxetic; Galerkin; graphene origami; nonlinear vibration

1. Introduction

Circular cylindrical shells are widely utilized in different industries, like aerospace, automotive, marine structures, different biomedical applications, etc., due to their low weight due to their limited thickness (Lvov *et al.* 2022) and (Lee 2009). Therefore, the importance of analyzing and studying this structure to improve its performance and optimize its design has always been considered, because dynamic loading in the long term can lead to defects and problems, some of which are resonance or amplification, which itself causes an increase in unwanted and destructive vibrations in the system, structural fatigue, which will have long-term implications on the strength, health, and stability of the structure, and, as a result, will create higher costs for construction and maintenance operations. In order to prevent these defects, performing accurate and correct dynamic analyses, using optimization methods, evaluating energy sources, and using appropriate and modern materials, as well as improving the safety level of structures, are of great importance in various articles done by Pasternak *et al.* (2022).

Composite cylindrical shells with their novel properties, like lower weight and higher resistance, are one of the most useful structures in the recent decades, so the researchers aim to develop this structure to find them more useful. Srinivas (1974) has been produced an advanced theory for the static and dynamic evaluations of finite, layered, composite material, circular cylindrical shells with any kind of boundary conditions, a specific three-dimensional analysis of simply supported shells. So based on the opinion that shows in the composite shells with laminated structure the core material is rolled like the web in the I-beam and both face sheets are as a flange of it. Hence the core material is one of the most fundamental causes of discussion and reviews by Guo *et al*. (2020), Wang *et al.* (2020) and Gomes *et al*. (2023), for having more stability and dynamic resistance, the researchers produce the novel kind of metamaterial, which is auxetics as a core in these structures. A multitude of studies on composite constructions has been published in the past few years, Auxetic materials are innovative designs that demonstrate unique behavior; these materials contain a NPR, indicating that when stretched, they expand subsequently. Consequently, this uncommon behavior has led to the reporting of numerous beneficial features via Ren *et al*. (2018a). Because of their exceptional characteristics, like extremely lightweight, strength-to-weight ratio, noise reduction, and great energy absorption capability, they are extensively utilized throughout several domains. Medical devices employ auxetic materials because of their excellent resistance against deformation which is reported by Duncan *et al.* (2018) and Allen *et al.* (2017). Mardling *et al*. (2020) have also stated that the application of auxetic frameworks can restore the characteristics of biological materials and utilize auxetic

*Corresponding author, Ph.D.,
E-mail: febrahimy@eng.ikiu.ac.ir

ISSN: 2287-237X (Print), 2287-2388 (Online)

materials in biomedical engineering technologies and biological gadgets. Additionally, auxetic materials are characterized by their being adaptable and flexible, and when made of sensitive substances, they respond to the environment (Papadopoulou *et al.* 2017*)*. For instance, like to other forms of metamaterials, the NPR of auxetics typically results directly from the topology of their nano/ micro-architecture. Consequently, Kolken and Zadpoor (2017) concentrate on the topology-property link within three primary categories of auxetic metamaterials like re-entrant, anti-chiral, and rotating (semi-) solid structures. Moreover, Ren *et al.* (2018b) indicated that auxetic materials exhibit exceptional capabilities, only a limited number have been manufactured and utilized in actual applications. This part outlines limitations and future directions in auxetics to stimulate potential research activities. Auxetic metamaterials, characterized by their lightweight properties, possess possible applications across various domains, including civil engineering, aerospace, and automotive engineering. Aso, to enhance the energy absorption without losing weight and other properties, Han *et al.* (2018), Carneiro *et al.* (2013), Lim (2015) and Mir *et al.* (2014) studied this novel auxetic structures that mentioned.

As a core for composite laminated shells, auxetics are perfect to approach more stability with less weight; Furthermore, Gupta and Pradyumna (2022) have studied on these structures in the past years. The research investigation examines the dynamic nonlinear motion of sandwich panels incorporating an auxetic honeycomb core and skin sheets made of composite materials with curved fibers for the first time. Chen and Ma (2024) examined the free oscillation and damping properties of carbon fiber-reinforced laminated cylindrical shells, including 3D re-entrant auxetic cores. The subsequent paper focuses on auxetic composites with fillers, exploring their categorizations, mechanical reactions, and fundamental principles. Additionally, it thoroughly examined several design aspects that affect the operation of auxetic-cores composites and balances them with traditional counterparts regarding mechanisms and mechanical properties by Hu *et al.* (2024). The dynamics of a circular cylindrical shell carrying a rigid disk on the top and clamped at the base are investigated as well done by Pellicano and Avramov (2007). A mathematical A approach has been proposed to examine the vibrational characteristics of a composite cylindrical shell subjected to moving internal pressure. The shell includes three layers, with the inner and outer layers exhibiting elastic and isotropic characteristics, while the center layer features a honeycomb construction consisting of a NPR. The Equations of motion have been determined by classical shell theory and Hamilton's principle (Eipakchi and Nasrekani 2020). A methodical approach is suggested for measuring the deformations of a composite cylindrical shell which includes a honeycomb core and various thicknesses subjected to multiple axial, internal, and outside stresses by Eipakchi, and Mahboubi (2022). The subsequent work examines the dynamic response and oscillation of laminated double-curved thin shells with NPR in an auxetic honeycomb core rest on elastic foundations, under the blast and damping loads by mathematical solutions (Duc *et al.* 2017*)*.

Cong *et al.* (2019) examined the nonlinear dynamics of stiffened round cylindrical shells with NPR in an auxetic honeycomb core layer, situated on Winkler foundations and exposed to mechanical loads. In addition, the Cong *et al.* (2018) study makes double-curved shallow shells with an auxetic core comprising three layers, where the top and bottom exterior sheets are constructed from isotropic aluminum, while the middle layer features a honeycomb shape utilizing the same aluminum material. An analytical method is proposed to examine the nonlinear dynamic study of porous eccentrically strengthened double-curved deep auxetic shells with a NPR under blast, mechanical, and thermal stresses, based on a Visco-Pasternak foundation model. The three-layer double-curved shallow shell comprises an auxetic honeycomb core layer with integrated not-Newtonian polymeric plastic and isotropic homogenous materials on the upper and lower surfaces. Additionally, the external surfaces of the PES-reinforced system are composed of functionally graded materials, and auxetic shells are situated in thermal places by Cong *et al.* (2021).

The integration of an auxetic core with face sheets constructed from modern composite materials significantly enhances the load capability of the structure. The study presents a novel design of auxetic circular shells featuring carbon nanotube-reinforced coatings. The nonlinear stability characteristics of circular shells containing carbon nanotube-reinforced coatings subjected to axial compressive loads are examined via Ly *et al*. (2024). A novel full-composite cylindrical shell with a foam-filled cavity lattice core has been created and produced with a nonlinear dynamic model that accounts for the amplitude-dependent characteristics of composite materials. The recommended nonlinear dynamic design could represent the lower vibrations and heightened resonance responses of structures exposed to initial periodic excitations, in contrast to conventional linear dynamic models by Dong *et al.* (2023). The nonlinear aeroelastic unreliability of a composites, composite shells exposed to ultrasonic airflow and thermal loads is investigated. The sandwich panel consists of three-phase composites including polymer/graphene platelet/fiber skins on the upper and lower surfaces and a honeycomb core layer demonstrating a negative Poisson's ratio (Karimiasl and Alibeigloo 2023). Their article aims to assess the dynamic behavior of sandwich toroidal shells featuring a core with a negative Poisson's coefficient and nanocomposite-enhanced coating layers subjected to reactive and periodic pressures, while accounting for geometrical nonlinearity. The obtained results indicate that the magnitude of exterior deformations significantly rises upon the suggested sandwich shells are exposed to regular periodic and rapid loadings, demonstrating the detrimental impacts of this type of dynamic loading by Mirfatah *et al.* (2024). The impact of the novel type of stiffeners and blast loads on the nonlinear dynamic reaction and oscillation of auxetic laminated honeycomb plates rest on Pasternak elastic substructure is examined by Cong *et al.* (2021). The most notable aspect is that the external sheets of the system, strengthened by lattice stiffeners (both orthogonal and diagonal), are

composed of materials with functional grades.

Graphene is an incredible material with many excellent reviews associated with it. It is the thinnest material known in creation and the strongest one ever recorded. The charge carriers demonstrate excellent inherent flexibility, possess no mass efficiency, and can traverse micrometers with no scattering at normal temperature. Graphene can endure current densities that are six orders of magnitude higher than Cu, has remarkable thermal insulation and rigidity, is resistant to gases, and harmonizes the seemingly contradictory properties of brittleness and flexibility (Cooper *et al.* 2012). Jiang *et al.* (2016) have focused on discovering more efficient coefficients in auxetic structures composed of graphene, leading to the continuous rise of these materials. Origami originates from a traditional form of art that transforms flat, thin surfaces into complex, three-dimensional structures. Currently, this transition surpasses art by providing a theoretical basis for non-destructive and scale-independent abstracts useful for engineering across several domains, potentially influencing education, research, and technology. A rising number of engineered materials and structures utilize origami principles, resulting in features that vary from those observed in both natural and artificial systems (Misseroni *et al.* 2024). Considering graphene and origami, a novel sort of auxetic known as Graphene Origami has been developed by Zhao *et al.* (2022). GOri facilitated metallic metamaterials are innovative materials that exhibit a NPR and superior mechanical characteristic, independent of the structure's topology or architecture. A method for approximating material properties using established micromechanical models, molecular dynamics (MD) simulations, and a genetic programming (GP) algorithm has been devised (Zhao *et al.* 2021). The GP-based Halpin-Tsai model is thoroughly trained using MD simulation data to accurately determine the Young's modulus of metamaterials across different GOri folding degrees, graphene amounts, and temperatures by (Zhao *et al.*2022).

Furthermore, on another study Hoang and Thanh (2025) examines the free oscillation and nonlinear dynamic response of functionally graded graphene origami-enabled auxetic metamaterial (GOEAM) cylindrical shells under thermal conditions. The multilayered shells feature GOri distributions across their thickness, introducing distinct auxetic and thermal properties. Vibrational behavior and static bending analysis the shear deformability of a cylindrical shell is examined in many articles utilizing Hamilton's principle. The shell is produced using a Cu core reinforced with GOri metamaterial and is exposed to external stresses. Fang *et al.* (2024) reported The graphene origami materials may be used in aerospace vehicles and structures and defense technology because of their low weight and high stiffness (Yang *et al.* 2024) and (Samadzadeh *et al.* 2024). Nonlinear dynamics analysis is an important factor for designing many useful structures and approximating their behavior. Against the external distributed or Concentrated force. In the subsequent work Dong *et al.* (2023) examines the analytical approach to post-buckling behavior in torsion-loaded sandwich carbon nanotube (CNT) reinforced cylindrical shells featuring an auxetic core. A cylindrical sandwich incorporating a double arrowed auxetic structure is presented, and its dynamic behavior is examined by Gao *et al.* (2020). An extensive analysis of their mechanical properties is essential. This research investigates the free vibration properties of a three-layer circular shell filled with fluid. The core layer of this construction incorporates a re-entrant honeycomb auxetic configuration, whereas the inner and outer layers are presumed to be isotropic and fabricated from aluminum (Khorshidi *et al.* 2025) and (Wang *et al.* 2010).

The nonlinear dynamics of a polymer cylindrical shell with a top mass under axial periodic excitation are investigated experimentally by Zippo *et al.* (2020). Amabibi *et al*. (1999) conducted an examination of the non-linear dynamics and buckling of simply supported circular cylindrical shells carrying transparent incompressible fluid flow. In the another research Li and Fu (2022) concentrated on the vibration analysis of auxetic sandwich cylindrical shell structures supported by an elastic basis. Zhang *et al.* (2012) study examined the nonlinear vibrations of a laminate layered cylindrical shell, which is clamped along a generatrix and features radially pre-stretched sheets at both ends, for the first time. The dynamic influence of the membrane on the circular cylindrical shell is substituted by a nonlinear elastic excite with damping.

Ebrahimi and Dadashi (2023) examined the oscillation analysis of a sandwich cylindrical shell including a honey comb core with a NPR, exposed to pre-loaded axial compression and external excitation forces. The equations governing the motion are derived using Donnell's enhanced shell theory, neglecting the thickness of cylindrical shells, and the dynamical analysis of shells is conducted using Galerkin's approach. Their article aims to examine the linear and nonlinear characteristics of the structure's oscillation. Additionally, various parametric examples are given and analyzed to demonstrate the impact of different parameters on the vibration of the three-layer cylindrical shell.

Considering all the studies mentioned and their review and study in this research, we intend to examine the linear and nonlinear dynamic response and vibration amplitude of this structure by adopting a newer type of anti-elastic material, called origami graphene, which was discussed earlier, as the main core material of the composite cylindrical shell under our study. We also intend to approach the linear and nonlinear dynamic response and vibration amplitude of this structure in addition to the geometric characteristics affecting the oscillations of this shell, such as axial preload and external driving load. Also, by making changes in the factors influencing the Poisson's ratio of the core, such as the percentage of hydrogen, which is related to the degree of folding and consequently the degree of negativity in the Poisson's ratio, or the weight fractions of origami graphene relative to the copper in the core, we will also witness a change in the vibration behavior and nonlinear dynamic response of the structure, which we will discuss in more detail below. An important and notable point in this research compared to previous studies is the change in the material and structure of the auxetic core, which we predict will have a substantial impact on improving the performance of the structure.

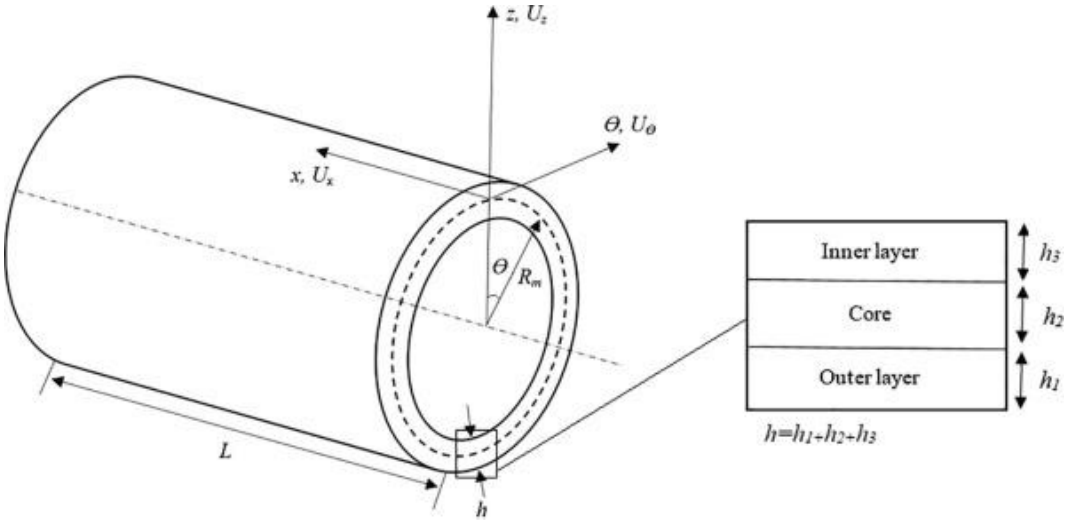

Fig. 1 The diagram of the composite cylindrical shell reinforced with origami graphene cores

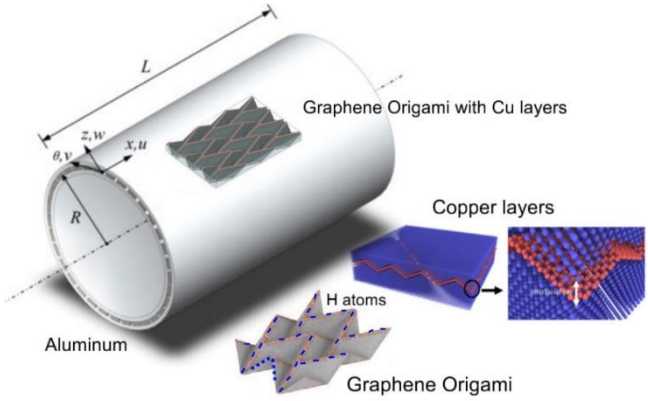

Fig. 2 The diagram of the laminated composite cylindrical shell reinforced with graphene origami enhanced with copper cores

2. The mathematical formulas

2.1 Face sheet material properties

This research examines a three-layered cylindrical shell comprising top and bottom outer layers of aluminum, with a core made of auxetic materials exhibiting an auxetic behavior. The thickness of the auxetic core is suggested $3 \times 10^{-3} m$.

Fig. 1 illustrates the configuration of a laminated cylindrical shell of three separate layers with specified thickness. Every point on the shell could be characterized using the cylindrical coordinate system (r, θ, z) by three parameters r, θ, and z. where r and θ refer to the axial and radial orientations of the shell, accordingly, and z is horizontal to the surface.

2.2 Auxetic mechanical properties

2.2.1 Graphene Origami

This research examines a cylindrical shell with an auxetic core composed of graphene origami, as illustrated in Fig. 2. The mechanical properties are articulated by micro-mechanical models and Genetic Programming (GP) as follows (Zhao *et al.* 2021):

$$E^{Gori} = E_{Cu}\frac{1+\xi\eta V_{Gr}}{1-\eta V_{Gr}} f_E(H_{Gr}, V_{Gr}, T) \tag{1}$$

$$\nu^{Gori} = (V_{Gr}\nu_{Gr} + V_{Cu}\nu_{Cu}) f_\nu(H_{Gr}, V_{Gr}, T) \tag{2}$$

$$\alpha^{Gori} = (V_{Gr}\alpha_{Gr} + V_{Cu}\alpha_{Cu}) f_\alpha(V_{Gr}, T) \tag{3}$$

$$\rho^{Gori} = (V_{Gr}\rho_{Gr} + V_{Cu}\rho_{Cu}) f_\rho(V_{Gr}, T) \tag{4}$$

In which:

$$f_E(H_{Gr}, V_{Gr}, T) = \begin{pmatrix} 1.11 - 1.22V_{Gr} - 0.134\left(\frac{T}{T_0}\right) + 0.559V_{Gr}\left(\frac{T}{T_0}\right) \\ -5.5H_{Gr}V_{Gr} + +38H_{Gr}V_{Gr}^2 - 20.6H_{Gr}^2V_{Gr}^2 \end{pmatrix} \tag{5}$$

$$f_\nu(H_{Gr}, V_{Gr}, T) = \begin{pmatrix} 1.01 - 1.43V_{Gr} + 0.165\left(\frac{T}{T_0}\right) - 16.8H_{Gr}V_{Gr} \\ -1.1H_{Gr}V_{Gr}\left(\frac{T}{T_0}\right) + +16H_{Gr}^2V_{Gr}^2 \end{pmatrix} \tag{6}$$

$$f_\alpha(V_{Gr}, T) = \begin{pmatrix} 0.794 - 16.8V_{Gr}^2 - 0.0279\left(\frac{T}{T_0}\right)^2 \\ +0.182\left(\frac{T}{T_0}\right)(V_{Gr}+1) \end{pmatrix} \tag{7}$$

$$f_\rho(V_{Gr}, T) = \left(1.01 - 2.01V_{Gr}^2 - 0.0131\left(\frac{T}{T_0}\right)\right) \tag{8}$$

Here is the volume fraction of graphene origami and copper based.

$$V_{Gr} = \frac{\rho_{Cu} W_{Gr}}{\rho_{Cu} W_{Gr} + \rho_{Gr}(1 - W_{Gr})} \tag{9}$$

$$V_{Cu} = 1 - V_{Gr} \tag{10}$$

The material coefficient is:

$$\eta = \frac{\frac{E_{Gr}}{E_{Cu}} - 1}{\frac{E_{Gr}}{E_{Cu}} + \xi} \tag{11}$$

And the size coefficient is:

$$\xi = 2\left(\frac{l_{Gr}}{t_{Gr}}\right) \tag{12}$$

The pattern of graphene origami designed will be in two different form, Uniform distribution pattern (U-W_{Gr}) and symmetrical distributed pattern (X-W_{Gr}), as shown below:

$$V_{Gr}(z) = V_{Gr} \quad \text{for (U-W}_{Gr}\text{)} \tag{13}$$

$$V_{Gr}(k) = \frac{2V_{Gr}|2k - N_L - 1|}{N_L}, k = 1,2,\ldots,N_L \quad \text{for (X-W}_{Gr}\text{)} \tag{14}$$

2.3 Kinematic formulations

Based on Donnell's improved shell theory for the motion eqautions will be in the form below Ebrahimi and Dadashi (2023):

$$\begin{aligned} \varepsilon_x &= \varepsilon_x^0 - z\chi_x \\ \varepsilon_\theta &= \varepsilon_\theta^0 - z\chi_\theta \\ \gamma_{x\theta} &= \gamma_{x\theta}^0 - 2z\chi_{x\theta} \end{aligned} \tag{15}$$

In which:

$$\begin{aligned} \varepsilon_x^0 &= \frac{\partial u}{\partial x} + \frac{1}{2}\left(\frac{\partial w}{\partial x}\right)^2 \\ \varepsilon_\theta^0 &= \frac{\partial v}{\partial \theta} - \frac{w}{R} + \frac{1}{2}\left(\frac{\partial w}{\partial \theta}\right)^2 \\ \gamma_{x\theta}^0 &= \frac{\partial v}{\partial x} + \frac{\partial u}{\partial \theta} + \frac{\partial w}{\partial x}\frac{\partial w}{\partial \theta} \end{aligned} \tag{16}$$

And also:

$$\begin{aligned} \chi_x &= \frac{\partial^2 w}{\partial x^2} \\ \chi_\theta &= \frac{1}{R}\frac{\partial v}{\partial \theta} + \frac{\partial^2 w}{\partial \theta^2} \\ \chi_{x\theta} &= \frac{1}{2R}\frac{\partial v}{\partial x} + \frac{\partial^2 w}{\partial x \partial \theta} \end{aligned} \tag{17}$$

ε_x^0 and ε_θ^0 represent the normal strains, while $\gamma_{x\theta}^0$ denotes the shear strain at the midsurface of the shell. Furthermore, the curvatures and twists can be defined by χ_x, χ_θ and $\chi_{x\theta}$. Hooke's law is employed to get the strain-stress Eq.s defined below for a cylindrical shell:

$$\begin{aligned} \sigma_x &= \frac{E}{1 - \nu^2}(\varepsilon_x + \nu\varepsilon_\theta) \\ \sigma_\theta &= \frac{E}{1 - \nu^2}(\varepsilon_\theta + \nu\varepsilon_x) \\ \sigma_{x\theta} &= \frac{E}{2(1 + \nu)}\gamma_{x\theta} \end{aligned} \tag{18}$$

The subsequent equation establishes the internal force and, consequently, the motion relevant to the shell concerning stressed components limited by thickness:

$$\begin{aligned} (N_i, M_i) &= \int_{\frac{-h}{2}}^{\frac{-h}{2+h_{al}^b}} \sigma_i^{al}(1, z)dz \\ &+ \int_{\frac{-h}{2}+h_{al}^b}^{\frac{-h}{2+h_{al}^b+h_a}} \sigma_i^{a}(1, z)dz + \int_{\frac{-h}{2+h_{al}^b+h_a}}^{\frac{-h}{2+h_{al}^b+h_a+h_{al}^t}} \sigma_i^{al}(1, z)dz \end{aligned} \tag{19}$$

The thickness of the bottom outside skin, auxetic core, and higher outer layer are denoted by h_{al}^b, h_a and h_{al}^t correspondingly, in the previously described equations, as seen in Fig. 1.

The subsequent relations are established by substituting the preceding formulas into Eq. (19):

$$\begin{bmatrix} N_x \\ N_\theta \\ N_{x\theta} \\ M_x \\ M_\theta \\ M_{x\theta} \end{bmatrix} = \begin{bmatrix} A_{11} & A_{12} & 0 & B_{11} & B_{12} & 0 \\ A_{12} & A_{22} & 0 & B_{12} & B_{22} & 0 \\ 0 & 0 & A_{66} & 0 & 0 & B_{66} \\ B_{11} & B_{12} & 0 & D_{11} & D_{12} & 0 \\ B_{12} & B_{22} & 0 & D_{12} & D_{22} & 0 \\ 0 & 0 & B_{66} & 0 & 0 & D_{66} \end{bmatrix} \begin{bmatrix} \varepsilon_x^0 \\ \varepsilon_\theta^0 \\ \gamma_{x\theta}^0 \\ -\chi_x \\ -\chi_\theta \\ -2\chi_{x\theta} \end{bmatrix} \tag{20}$$

The A_{ij}, B_{ij} and D_{ij} will be defined as follow:

$$\begin{aligned} \begin{bmatrix} A_{ij} \\ B_{ij} \\ D_{ij} \end{bmatrix} &= \int_{\frac{-h}{2}}^{\frac{-h}{2+h_{al}^b}} Q_{ij}^{al} \begin{bmatrix} 1 \\ z \\ z^2 \end{bmatrix} dz + \int_{\frac{-h}{2}+h_{al}^b}^{\frac{-h}{2+h_{al}^b+h_a}} Q_{ij}^{a} \begin{bmatrix} 1 \\ z \\ z^2 \end{bmatrix} dz \\ &+ \int_{\frac{-h}{2+h_{al}^b+h_a}}^{\frac{-h}{2+h_{al}^b+h_a+h_{al}^t}} Q_{ij}^{al} \begin{bmatrix} 1 \\ z \\ z^2 \end{bmatrix} dz \end{aligned} \tag{21}$$

Where:

$$\begin{aligned} Q_{11}^{al} &= Q_{22}^{al} = \frac{E_{al}}{1 - \nu_{al}^2}, \qquad Q_{12}^{al} = \frac{E_{al}\nu_{al}}{1 - \nu_{al}^2}, \\ Q_{66}^{al} &= \frac{E_{al}}{2(1 + \nu_{al})}, \qquad Q_{11}^{a} = Q_{22}^{a} = \frac{E_1^{(c)}}{1 - \nu_{12}^c \nu_{21}^c}, \\ Q_{12}^{a} &= \frac{E_2^{(c)}\nu_{12}^{(c)}}{1 - \nu_{12}^c \nu_{21}^c}, \qquad Q_{66}^{a} = \frac{E_2^{(c)}}{2\left(1 + \nu_{12}^{(c)}\right)} \end{aligned} \tag{22}$$

The governed Eq. of motion of the cylindrical shell will be defined as:

$$\begin{aligned} \frac{\partial N_x}{\partial x} + \frac{\partial N_{x\theta}}{\partial \theta} &= \rho_1 \frac{\partial^2 u}{\partial t^2} \\ \frac{\partial N_{x\theta}}{\partial x} + \frac{\partial N_\theta}{\partial \theta} - \frac{1}{R}\left(\frac{\partial M_{x\theta}}{\partial x} + \frac{\partial M_\theta}{\partial \theta}\right) &= \rho_1 \frac{\partial^2 v}{\partial t^2} \end{aligned} \tag{23}$$

$$\frac{\partial^2 M_x}{\partial x^2}+2\frac{\partial^2 M_{x\theta}}{\partial x\partial\theta}+\frac{\partial^2 M_\theta}{\partial\theta^2}+\frac{N_x}{R}+\frac{\partial}{\partial x}\left(N_x\frac{\partial w}{\partial x}+N_{x\theta}\frac{\partial w}{\partial\theta}\right)+\frac{\partial}{\partial\theta}\left(N_{x\theta}\frac{\partial w}{\partial x}+N_\theta\frac{\partial w}{\partial\theta}\right)-ph\frac{\partial^2 w}{\partial x^2}+q=\rho_1\frac{\partial^2 w}{\partial t^2}+2\varepsilon\rho_1\frac{\partial w}{\partial t}$$

In which ε denoted the Damping coefficient, p is the axial pre-load and q is stand for the distributed force.

That the mass inertia is:

$$\rho_1=\int_{-\frac{h}{2}}^{\frac{h}{2}}\rho dz \tag{24}$$

By putting Eqs. (16 -17) into the Eq. (20) and replacing them into the Eqs. (23), the final governing equations of cylindrical shell will be defined as below:

$$\begin{aligned}&l_{11}(u)+l_{12}(v)+l_{13}(w)+P_1(w)=\rho_1\frac{\partial^2 u}{\partial t^2}\\&l_{21}(u)+l_{22}(v)+l_{23}(w)+P_2(w)=\rho_1\frac{\partial^2 v}{\partial t^2}\\&l_{31}(u)+l_{32}(v)+l_{33}(w)+P_3(w)+Q_3(u,w)+R_3(v,w)-ph\frac{\partial^2 w}{\partial x^2}+q=\rho_1\frac{\partial^2 w}{\partial t^2}+2\varepsilon\rho_1\frac{\partial w}{\partial t}\end{aligned} \tag{25}$$

To find more information about l_{ij} see also Appendix 1.

3. Solving equations

3.1 Solution method

In this article we used the Galerkine approach to solve the Eq.s, considering this and based on the Simply-Supported boundary conditions at both end and also initial conditions the approximated answer to this system will be in the following form:

$$w=0,\ v=0,\ M_x=0 \quad \text{(Simply-Supported boundary conditions)} \tag{26}$$

$$\begin{aligned}u&=U(t)\cos\frac{m\pi x}{L}\sin\frac{n\theta}{R},\\v&=V(t)\sin\frac{m\pi x}{L}\cos\frac{n\theta}{R}\\w&=W(t)\sin\frac{m\pi x}{L}\sin\frac{n\theta}{R}\end{aligned} \tag{27}$$

In which the U, V and W stand for the amplitude of vibration and m, n stand for half waves number in the axial and the circumferential directions in the respective order.

During the Galerkin procedure, by putting Eqs. (27) into Eqs. (25) the equaitons can be rewrite as follows:

$$\begin{aligned}&l_{11}U+l_{12}V+l_{13}W+n_1W^2=\rho_1\frac{d^2U}{dt^2}\\&l_{21}U+l_{22}V+l_{23}W+n_2W^2=\rho_1\frac{d^2V}{dt^2}\\&l_{31}U+l_{32}V+l_{33}W+n_3W^2+n_4W^3+n_5UW+n_6VW+\frac{16q}{\pi^2mn}=\rho_1\frac{d^2W}{dt^2}+2\varepsilon\rho_1\frac{dW}{dt}\end{aligned} \tag{28}$$

Checked Appendix 2 for more. Provided Volmir's assumptions is valid ($u\ll w$, $v\ll w$, $\rho_1\left(\frac{\partial^2 U}{\partial t^2}\right)\to 0$ and $\rho_1\left(\frac{\partial^2 V}{\partial t^2}\right)\to 0$) the governing Eq.s will be obtained as follow:

$$\begin{aligned}&l_{11}U+l_{12}V+l_{13}W+n_1W^2=0\\&l_{21}U+l_{22}V+l_{23}W+n_2W^2=0\\&l_{31}U+l_{32}V+l_{33}W+n_3W^2+n_4W^3+n_5UW+n_6VW+\frac{16q}{\pi^2mn}=\rho_1\frac{d^2W}{dt^2}+2\varepsilon\rho_1\frac{dW}{dt}\end{aligned} \tag{29}$$

Solving 1st and 2nd Eq. to find U and V in parametric form then put them into the 3rd Eq. and by factoring the same coefficients, the Eq. (29) will be turn into the following form.

$$\rho_1\frac{d^2W}{dt^2}+2\varepsilon\rho_1\frac{dW}{dt}+a_1W-a_2W^2+a_3W^3=\frac{16q}{\pi^2mn} \tag{30}$$

In which the a_1, a_2 and a_3 would be:

$$\begin{aligned}a_1&=-l_{33}-\frac{l_{31}(l_{12}l_{23}-l_{22}l_{13})+l_{32}(l_{21}l_{13}-l_{11}l_{23})}{l_{11}l_{22}-l_{12}^2}\\a_2&=n_3+\frac{n_5(l_{12}l_{23}-l_{22}l_{13})+n_6(l_{21}l_{13}-l_{11}l_{23})}{l_{11}l_{22}-l_{12}^2}+\frac{l_{31}(l_{12}n_2-l_{22}n_1)+l_{32}(l_{12}n_1-l_{11}n_2)}{l_{11}l_{22}-l_{12}^2}\\a_3&=-n_4-\frac{n_5(l_{12}n_2-l_{22}n_1)+n_6(l_{21}n_1-l_{11}n_2)}{l_{11}l_{22}-l_{12}^2}\end{aligned} \tag{31}$$

So, the approximate Eq. (30) will be utilized for the nonlinear dynamic analysis of cylindrical shells.

3.2 Natural frequency

If there is no external pressure like, pre-loads or any distributed forces the natural frequency of the structure will be calculated as follows:

$$\begin{vmatrix}l_{11}+\rho_1\omega^2 & l_{12} & l_{13}\\ l_{21} & l_{22}+\rho_1\omega^2 & l_{23}\\ l_{31} & l_{32} & l_{33}+\rho_1\omega^2\end{vmatrix}=0 \tag{32}$$

By solving Eq. (32) the three angular frequencies will obtained, the axial, the radial and the circumferential frequency, Hence the smallest one is chosen. Also based on Eq. (30) the approximated frequency could be calculated as below:

$$\omega_{mn}=\sqrt{\frac{a_1}{\rho_1}} \tag{33}$$

3.3 Amplitude to frequency ratio curve of nonlinear vibration

The nonlinear vibration of a circular cylindrical shell via considering the effects of distributed transvers load ($q = Q\ sin\ \Omega\ t$) and pre-load as well, is expressed as follows:

$$\rho_1 \frac{d^2W}{dt^2} + 2\varepsilon\rho_1 \frac{dW}{dt} + a_1 W - a_2 W^2 + a_3 W^3 - \frac{16Q}{\pi^2 mn} sin\ \Omega\ t = 0 \quad (34)$$

via dividing both sides by ρ_1 the Eq. (32) and considering the Eq. (31) we approached the below formula:

$$\frac{d^2W}{dt^2} + 2\varepsilon\frac{dW}{dt} + \omega_{mn}^2(W - GW^2 + JW^3) - F\ sin\ \Omega\ t = 0 \quad (35)$$

That the ω_{mn} is the natural frequency of the cylindrical shells, and the G, K and F will be defined as follow:

$$G = \frac{a_2}{a_1}\ ,\quad J = \frac{a_3}{a_1},\quad F = \frac{16Q}{\rho_1 \pi^2 mn} \quad (36)$$

Considering $W = A\ sin\ \Omega\ t$ and utilizing the Galerkine method and then multiply both sides by $(sin\ \Omega\ t)$ and then integrate both sides with regard to t from 0 to $\frac{\pi}{2\Omega}$, will achieve to:

$$\Omega^2 - \frac{4\varepsilon}{\pi}\Omega = \omega_{mn}^2\left(1 - \frac{8}{3\pi}GA + \frac{3J}{4}A^2\right) - \frac{F}{A} \quad (37)$$

If $\beta = \frac{\Omega}{\omega_{mn}}$, the Eq. (35) will be rewrite in the form of below:

$$\beta^2 - \frac{4\varepsilon}{\pi\omega_{mn}}\beta - \left(1 - \frac{8}{3\pi}GA + \frac{3J}{4}A^2\right) = -\frac{F}{A\omega_{mn}^2} \quad (38)$$

Without damping, the nonlinear oscillation of the shell will be:

$$\beta^2 - \left(1 - \frac{8}{3\pi}GA + \frac{3J}{4}A^2\right) = -\frac{F}{A\omega_{mn}^2} \quad (39)$$

If no external load(F=0) acting role in the nonlinear vibration formulas, the frequency ratio-amplitude relation of free nonlinear vibration will become as follow:

$$\Omega^2 = \omega_{mn}^2\left(1 - \frac{8}{3\pi}GA + \frac{3J}{4}A^2\right) \quad (40)$$

The frequency amplitude relations are defined used the Eq. (38) for cylindrical shells with graphene origami auxetic core.

3.4 Nonlinear dynamic responses

The nonlinear dynamic responses of circular cylindrical shells can be discovered utillizing the Eq. (30), By utilizing the fourth-order Runge-Kutta method, with the initial conditions ($y_0 = 0$) and also, change the variable to reduce this type of second-order differential Eq. to two first-order Eq.s, so we can define new variables in the following form:

Table 1 The efficiency parameters of CNTs

(*m*,*n*)	Bhimaraddi (1984)	Lam and Loy (1995)	Xuebin (2008)	Shen (2012)	Present
(1,1)	0.03692	0.0374	0.03739	0.03712	0.03760
(1,2)	0.03612	0.0367	0.03666	0.03648	0.03700
(1,4)	0.03632	0.0372	0.03723	0.03700	0.03770

Table 2 The nondimensional linear natural frequencies of composite cylindrical shells

n	Wang and Wu (2017)	Wang *et al.* (2019)	Present
2	1.2387	1.2425	1.2425
3	1.2325	1.2366	1.2367
4	1.2256	1.2300	1.2302

$$y_1 = W\ and\ y_2 = \frac{dW}{dt} \quad (41)$$

The nonlinear dynamic responses will be explained below:

$$\frac{dy_1}{dt} = y_2$$
$$\frac{dy_2}{dt} = \frac{1}{\rho_1}(-2\varepsilon y_2 - a_1 y_1 + a_2 {y_1}^2 - a_3 {y_1}^3 + \frac{16Q}{\pi^2 mn} sin\ \Omega\ t \quad (42)$$

4. Numerical data and analysis

In the present study, aluminum was used to model the upper and lower sheets of the composite shell, and origami graphene was used in the core of the structure. In addition, the geometric dimensions and sizes used are as follows:

$$L/R = 2, R/h = 200, m = 1, n = 3, Q = 1500, P = 0,$$
$$h_t = h_B = 0.001\ (m) h_c = 0.003\ (m)$$
$$E_{Al} = 69(GPa), \rho_{Al} = 2700\ (kg/m^3)\ ,$$
$$\nu_{Al} = 0.3\ ,\qquad E_{Cu} = 65.79(GPa),$$
$$\rho_{Cu} = 8800\ (kg/m^3)\ , \nu_{Cu} = 0.387$$
$$E_{Gr} = 929.57(GPa), \rho_{Gr} = 1800\ (kg/m^3)\ ,$$
$$\nu_{Gr} = 0.22\ , W_{Gr} = 2.5(wt\%)\ , H_{Gr} = 100\%$$

4.1 Validation

In this study, the dimensionless frequencies of isotropic cylindrical shells are determined and compared to previous references that are reported in Table 1. This is an additional attempt to confirm the validity of the findings. According to what is shown, the current findings are in perfect accord with the references mentioned in the table, which demonstrates that the results that were obtained are accurate.

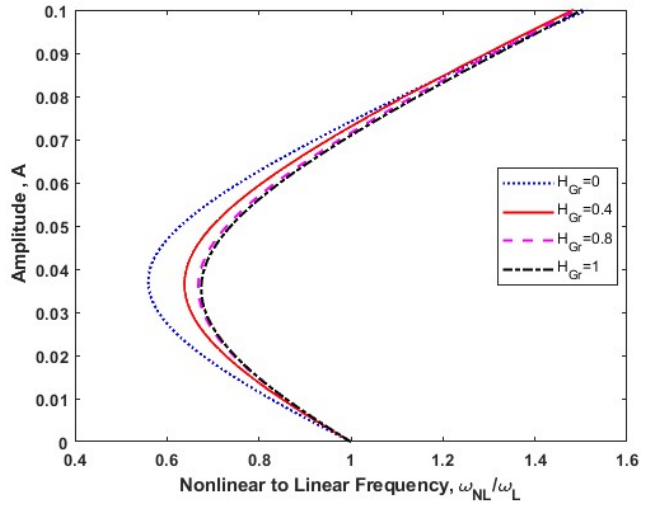

(a) The impact of different H_{Gr} on the nonlinear to the linear frequency-amplitude of circular cylindrical shell

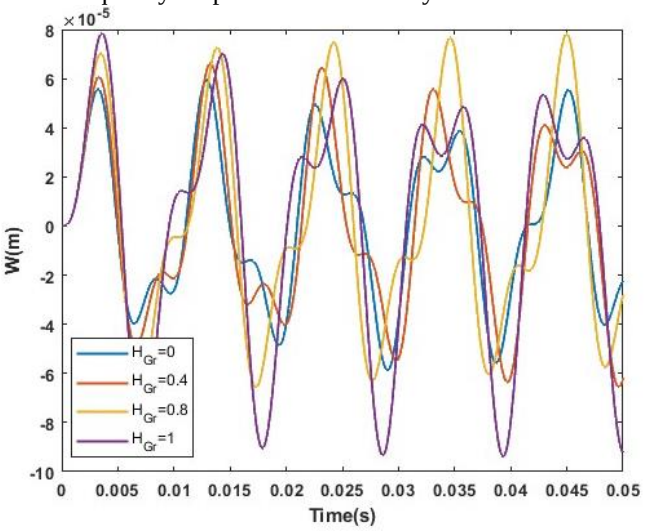

(b) The impact of various H_{Gr} on the Nonlinear responses of cylindrical shells

Fig. 3 The impact of various H_{Gr} on the amplitude-frequency and W-time curve

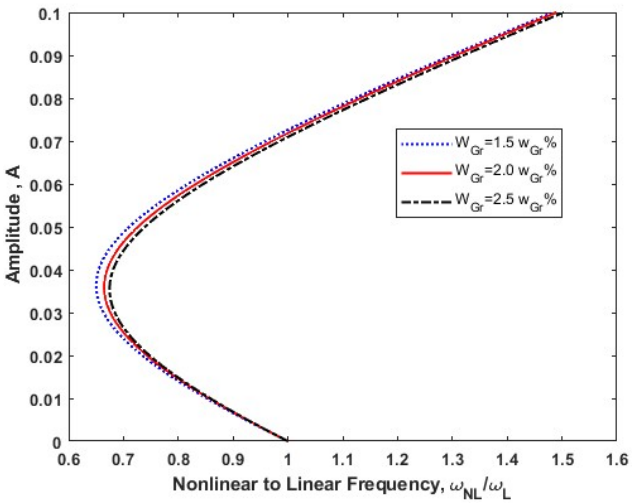

(a) The impact of different W_{Gr} on the nonlinear to the linear frequency-amplitude of circular cylindrical shell

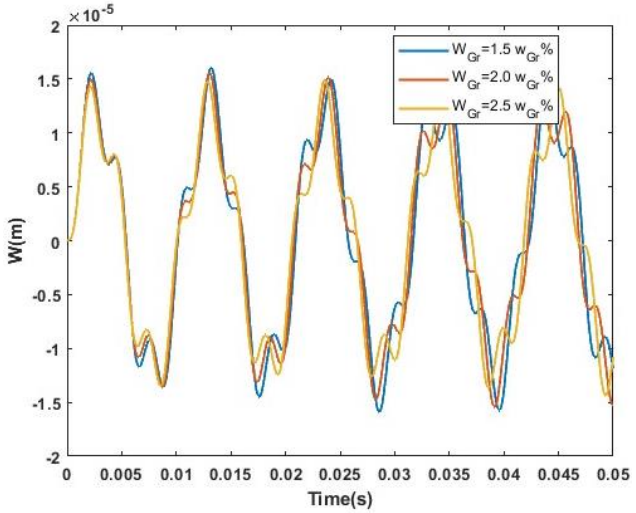

(b) The impact of various H_{Gr} on the Nonlinear responses of cylindrical shells

Fig. 4 The impact of various W_{Gr} on the amplitude-freqeancy and W-time curve

In this work, the nondimensional linear natural frequencies of composite cylindrical shells are compared with the nondimensional linear natural frequencies provided. The result of this compression is expressed in Table 2, which can be seen below. A comparison of the values stated in the references that were cited is presented in Table 2, which demonstrates that these values are in great agreement with those that have been stated in the literature.

4.2 Results and discussions

4.2.1 Core variables

Fig. 3(a) illustrates the impact of H_{Gr} on the nonlinear to the linear frequency versus amplitude curve of cylindrical shell with GOri core, it is obtained that the more Hydrogen percent on the graphene origami surface, the poisons ratio will be reduced and so the amplitude of vibration of the structure will become lower. For the nonlinear dynamis responses of the cylindrical shell it is the same as the previous, Fig. 3(a) illustrates the impact of various H_{Gr} of of the composite auxetic-core cylindrical shell's amplitude as a function of nonlinear versus linear frequency. The H_{Gr} percentage exhibits a reducing the influence on the amplitude of the vibration of the auxetic cylindrical shell due to its direct effect on the Poisson's ratio, which becomes more negative with higher H_{Gr} levels on the graphene origami surfaces. As the H_{Gr} grows, the vibration amplitude reduces. Furthermore, as the amplitude increases, the change from nonlinear to linear frequency reduces faster, and subsequent to the peak, it starts to rise with increasing amplitude. Furthermore, the minimum nonlinear to linear frequency starts to rise with an increase in H_{Gr}.

Fig. 3(b) gives the impact of the H_{Gr} percent on the W-t curve, as we can see W start to vibrate with time, it is notable that the amplitude of this oscillation increases as the H_{Gr} increase, as we know that the more H_{Gr} percent the less poisson's ratio we have so the auxetic behavior of the core is more. The most stability for the number of this core

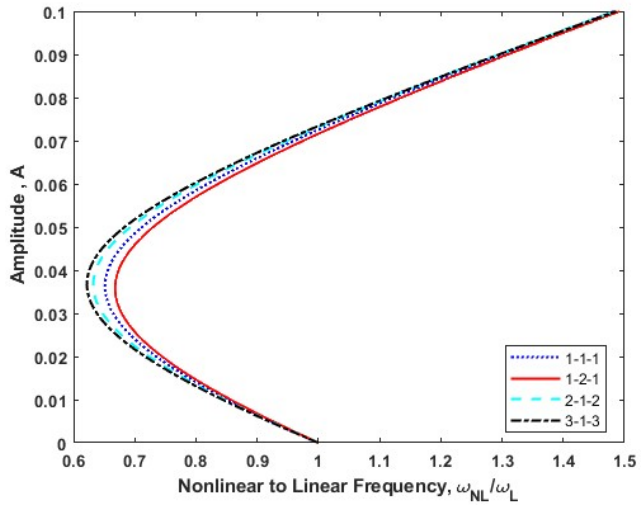

(a) The impact of various thickness on the nonlinear to the linear frequency-amplitude curve of cylindrical shell

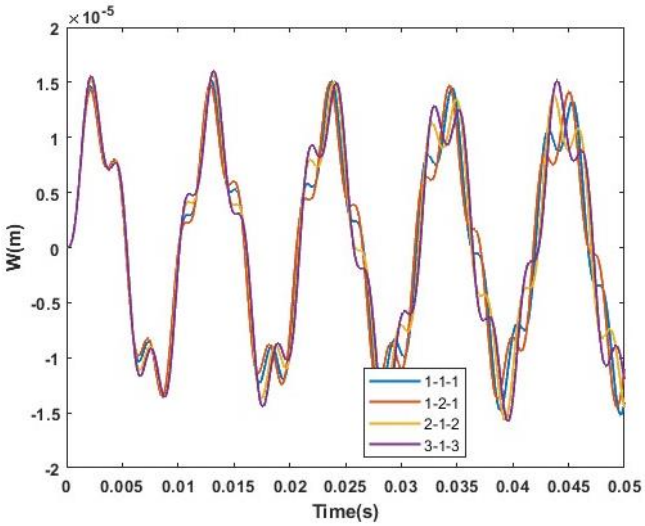

(b) The impact of various thickness on the Nonlinear responses of cylindrical shells

Fig. 5 The impact of various thickness on the Amplitude-frequancy and W-time curve

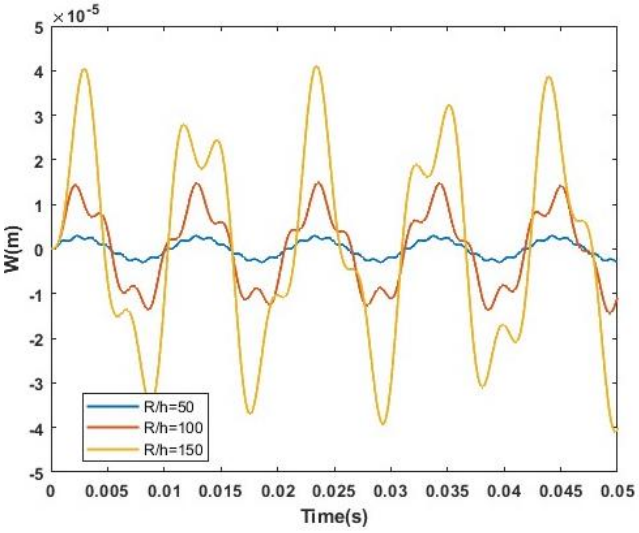

(a) The effect of various R/h on the Nonlinear responses of cylindrical shells

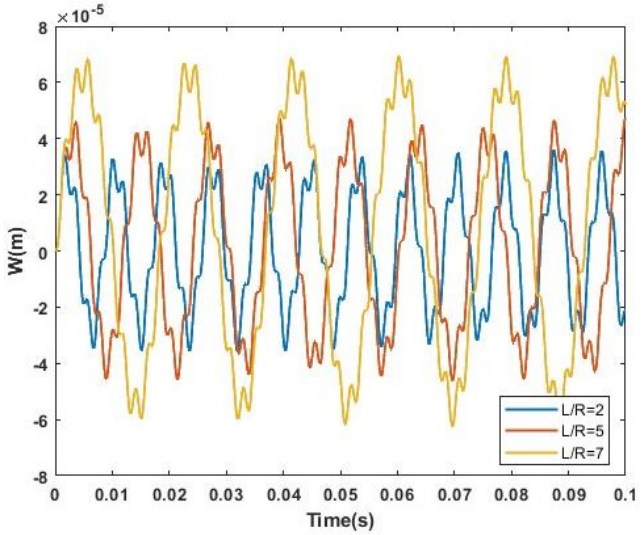

(b) The impact of various L/R on the Nonlinear responses of cylindrical shells

Fig. 6 The impact of various geometric parameters on the W-time curve

parameter is about 0.8.

Fig. 4(a) denote the effect of different W_{Gr} on the nonlinear to the linear frequency-amplitude curve of cylindrical shell with the an auxetic core, in which, on the contrary, the previous case via increasing the value of W_{Gr} the frequency ratio and amplitude of vibration will decrease. As it is easy to understand if W_{Gr} grows the more negative poisson's ratio we have. For the Fig.4(b) unlike the previous case, the weight fraction has the other effect on the W-time curve, in which via the more W_{Gr} like (W_{Gr}=2.5%) the less W at the beginning of the vibrate is shown. So, by controlling these two effective parameters, the Graphene origami is a kind of tunable auxetic metamaterial.

4.2.2 Geometrical variables

Fig. 5(a) specifically demonstrates the effect of various thickness of the cylindrical shell with an auxetic core on the nonlinear to linear frequency-amplitude curve. The greater the thickness of the auxetic core (1-2-1), the lower the ratio of nonlinear to linear frequency, according to the unique properties and more stiffness of the auxetic material. Moreover, this indicates that the auxetic material decreases the nonlinear frequencies of structures. In Fig. 5(b) the effects of different thickness are shown but as the same the more core thicknesses cause the less W value in the figure.

The effect of geometrical parameter is obviously expressed in the Fig. 6 (a,b) as illustrated in Fig. 6(a) as much as the cylindrical shell becomes more thicker the W would be reduce and by increasing the value of $^{R}/_{h}$ the shell become shallow shell and start to vibrate with higher W number. Fig. 6 (b) shows the impact of the $\frac{L}{R}$ on the W – time curve. it is obviously notable that the amplitude of these oscillations boosts as the $\frac{L}{R}$ ratio increases; this is

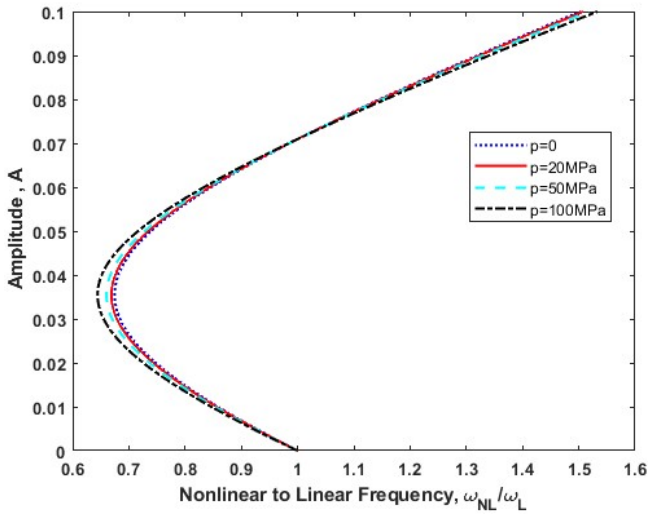

(a) The impact of different p on the nonlinear to the linear frequency-amplitude curve of composite shell

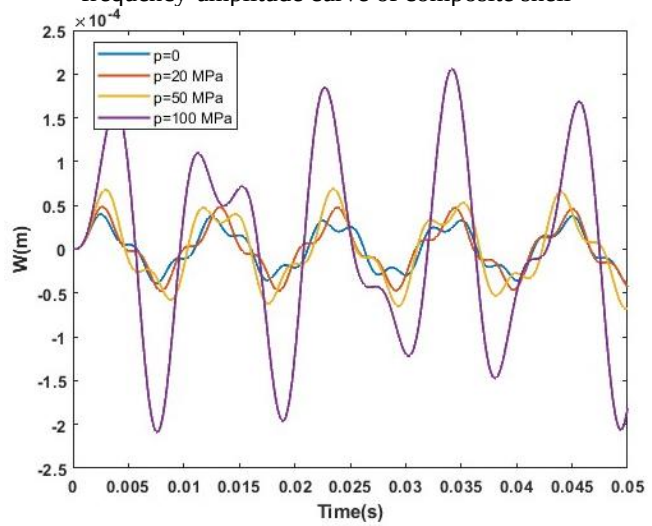

(b) The impact of various p on the Nonlinear responses of composite shells

Fig. 7 The impact of various pre-loaded on the Amplitude-frequency and W-time curve

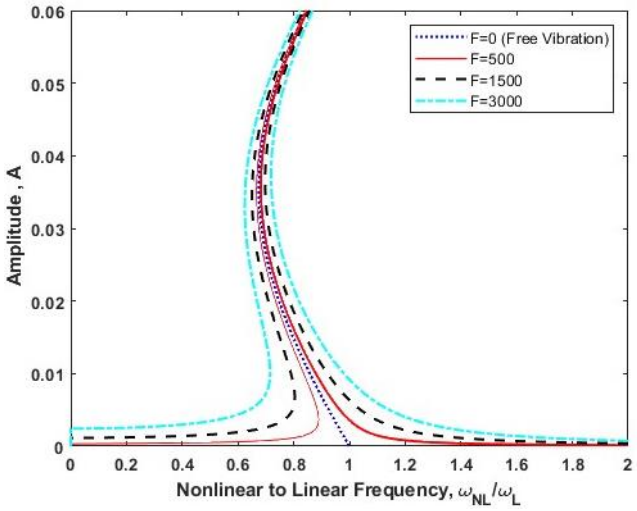

(a) The impact of different F on the nonlinear to the linear frequency-amplitude curve of cylindrical shell via an auxetic core

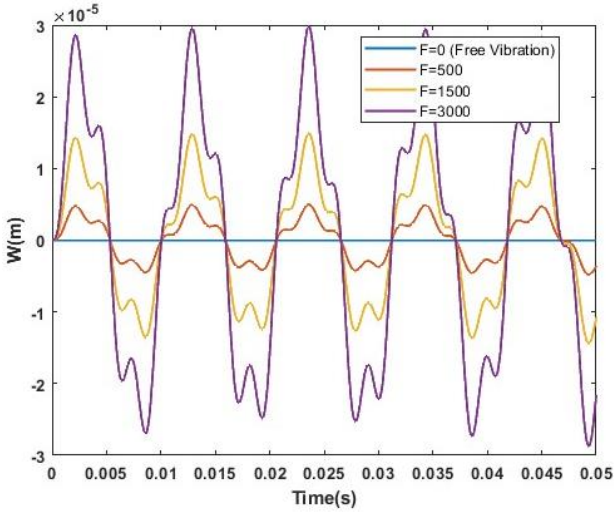

(b) The impact of various F on the Nonlinear responses of cylindrical shells

Fig. 8 The impact of various force on the Amplitude-frequency and W-time curve

completely justified by the structure of the laminated cylindrical shell, which the lesser the length of the cylindrical shell and the higher the radius of it, the better oscillation damped by the time.

4.2.3 External variables

The nonlinear to linear frequency-amplitude curves of the cylindrical shell and the effect of the axial pre-loaded are demonstrated in Fig. 7(a). The illustrated results show that the amplitude of vibration of the shells decreases as the value of load becomes more. In addition, it can be cause that the frequency value from nonlinear to linear initially reduces and begins to increase next to the peak. Furthermore, the minimum nonlinear to linear frequency reduces when the pre-loaded axial compression force increases.

The impact of pre-loaded axial compression on the W curve over time is investigated in Fig. 7(b). The total number of omega is subject to periodic oscillations, and it's obvious that a boost in p value results in greater amplitude of these oscillations.

Fig. 7(a) clearly illustrates that the rise in applied force corresponds with a heightened amplitude noticed at the beginning of motion. This shows that the force increasingly influences the amplitude, as predicted. Furthermore, as the amplitude grows, the graph of amplitude over nonlinear to linear frequency approaches the free vibration curve. Fig. 7(b) clarify the significant efficient cause of external force on dynamic responses; an increase in external load results in a greater W amplitude in the W-time curve.

Fig.8(a), (b) it shows that the more excitation at the beginning of the motion cause the higher amplitude of vibration as we expect, and by the time in Fig. 8(a) this curve tends into a free vibration because of the great absorption of auxetic core. Fig.8(b) illustrated that the

external distributed force is important for the controlling and approximate the nonlinear behavior of the structures

5. Conclusions

Considering the above-mentioned issues and citing previous research, in this study we have realized the importance of using anti-elastic materials in the core of multilayer composites, especially for controlling and improving vibrations. Then, by examining and analyzing numerical data, we found that in general:

• Geometric variables have a significant effect on controlling vibrations in this structure. The shorter the length of the cylindrical shell and the greater the radius of it, the better it absorbs vibrations by the time and also the thicker shells are the better vibration controlling and damping structures.

• Changes in the mechanical properties of auxetic materials also lead to a reduction in vibrations by changing the Poisson's ratio of the material. The more H_{Gr} and W_{Gr} cause the less poisson's ratio and the auxetic properties will becomes more efficient.

• External factors can also change the results of structural oscillations.

• Finally, it can be said that auxetic materials would be introduced as an effective core in sensitive structures and can be effective in various applications. In this case the Graphene Origami is one of the most and easily tunable one, which is enhanced the properties because of the effect of the graphene like more stiffness and low weight and the unique application of origami structures.

References

Allen, T., Hewage, T., Newton-Mann, C., Wang, W., Duncan, O. and Alderson, A. (2017), "Fabrication of auxetic foam sheets for sports applications", *Physica Status Solidi (B)*, **254**(12), 1700596. https://doi.org/10.1002/pssb.201700596.

Amabili, M., Pellicano, F. and Païdoussis, M.P. (1999), "Non-linear dynamics and stability of circular cylindrical shells containing flowing fluid. Part I: Stability", *J. Sound Vib.*, **225**(4), 655-699. https://doi.org/10.1006/jsvi.1999.2232.

Bhimaraddi, A. (1984), "A higher order theory for free vibration analysis of circular cylindrical shells", *Int. J. Solids Struct.*, **20**(7), 623-630. https://doi.org/10.1016/0020-7683(84)90064-0.

Carneiro, V.H., Meireles, J. and Puga, H. (2013), "Auxetic materials—A review", *Mater. Sci.*, **31**, 561-571. https://doi.org/10.2478/s13536-013-0021-3.

Chen, Y.L. and Ma, L. (2024), "Free vibration and damping characteristics of carbon-fiber-reinforced sandwich cylindrical shells with 3D reentrant auxetic core", *Mech. Adv. Mater. Struct.*, **31**(25), 6541-6552. https://doi.org/10.1080/15376494.2024.2199458.

Cong, P.H. and Duc, N.D. (2021), "Nonlinear dynamic analysis of porous eccentrically stiffened double curved shallow auxetic shells in thermal environments", *Thin Wall. Struct.*, **163**, 107748. https://doi.org/10.1016/j.tws.2021.107748.

Cong, P.H., Khanh, N.D., Khoa, N.D. and Duc, N.D. (2018), "New approach to investigate nonlinear dynamic response of sandwich auxetic double curves shallow shells using TSDT", *Compos. Struct.*, **185**, 455-465. https://doi.org/10.1016/j.compstruct.2017.12.063.

Cong, P.H., Long, P.T., Van Nhat, N. and Duc, N.D. (2019), "Geometrically nonlinear dynamic response of eccentrically stiffened circular cylindrical shells with negative Poisson's ratio in auxetic honeycombs core layer", *Int. J. Mech. Sci.*, **152**, 443-453. https://doi.org/10.1016/j.ijmecsci.2018.11.036.

Cong, P.H., Quyet, P.K. and Duc, N.D. (2021), "Effects of lattice stiffeners and blast load on nonlinear dynamic response and vibration of auxetic honeycomb plates", *Proceedings of the Institution of Mechanical Engineers, Part C: Journal of Mechanical Engineering Science*, **235**(23), 7192-7211. https://doi.org/10.1177/0954406220983329.

Cooper, D.R., D'Anjou, B., Ghattamaneni, N., Harack, B., Hilke, M., Horth, A., Majlis, N., Massicotte, M., Vandsburger, L., Whiteway, E. and Yu, V. (2012), "Experimental review of graphene", *Int. Scholar. Res. Not.*, **2012**(1), 501686. https://doi.org/10.5402/2012/501686.

Dong, B., Li, H., Li, K., Zhang, F., Qiao, Z., Yang, Y., Deng, Y., Wang, S., Bai, H., Zhang, H. and Cao, H. (2023), "Nonlinear dynamic modeling and experimental study of full-composite cylindrical shells with a foam-filled cavity lattice core", *Nonlinear Dyn.*, **111**(22), 20899-20927. https://doi.org/10.1007/s11071-023-08295-0.

Dong, D.T., Phuong, N.T., Nam, V.H., Ly, L.N., Tien, N.V., Duc, V.M., Minh, T.Q., Hung, V.T. and Giang, N.T.H. (2023), "An analytical approach for nonlinear buckling analysis of torsionally loaded sandwich carbon nanotube reinforced cylindrical shells with auxetic core", *Adv. Appl. Math. Mech.*, **15**, 468-484. https://doi.org/10.4208/aamm.OA-2022-0154

Duc, N.D., Seung-Eock, K., Cong, P.H., Anh, N.T. and Khoa, N.D. (2017), "Dynamic response and vibration of composite double curved shallow shells with negative Poisson's ratio in auxetic honeycombs core layer on elastic foundations subjected to blast and damping loads", *Int. J. Mech. Sci.*, **133**, 504-512. https://doi.org/10.1016/j.ijmecsci.2017.09.01.

Duncan, O., Shepherd, T., Moroney, C., Foster, L., Venkatraman, P. D., Winwood, K., Allen, T. and Alderson, A. (2018), "Review of auxetic materials for sports applications: Expanding options in comfort and protection", *Appl. Sci.*, **8**(6), 941. https://doi.org/10.3390/app8060941.

Ebrahimi, F. and Dadashi, M. (2023), "Composite cylindrical shells with auxetic core on elastic foundation: A nonlinear dynamic analysis", *Structures*, **57**, 105170. https://doi.org/10.1016/j.istruc.2023.105170.

Eipakchi, H. and Mahboubi Nasrekani, F. (2022), "Axisymmetric analysis of auxetic composite cylindrical shells with honeycomb core layer and variable thickness subjected to combined axial and non-uniform radial pressures", *Mech. Adv. Mater. Struct.*, **29**(12), 1798-1812. https://doi.org/10.1080/15376494.2021.1976808.

Eipakchi, H. and Nasrekani, F.M. (2020), "Vibrational behavior of composite cylindrical shells with auxetic honeycombs core layer subjected to a moving pressure", *Compos. Struct.*, **254**, 112847. https://doi.org/10.1016/j.compstruct.2020.112847.

Fang, K., Huang, G., Yu, G., Xu, W. and Yuan, W. (2024), "Free vibration analysis of graphene origami-reinforced nano cylindrical shell", *Mech. Adv. Mater. Struct.*, **31**(29), 12099-12111. https://doi.org/10.1080/15376494.2024.2212341.

Gao, Q., Liao, W.H. and Huang, C. (2020), "Theoretical predictions of dynamic responses of cylindrical sandwich filled with auxetic structures under impact loading", *Aerosp. Sci. Technol.*, **107**, 106270. https://doi.org/10.1016/j.ast.2020.106270.

Gomes, R.A., de Oliveira, L.A., Francisco, M.B. and Gomes, G.F. (2023), "Tubular auxetic structures: A review", *Thin Wall. Struct.*, **188**, 110850. https://doi.org/10.1016/j.tws.2023.110850.

Guo, Y., Zhang, J., Chen, L., Du, B., Liu, H., Chen, L., Li, W. and Liu, Y. (2020), "Deformation behaviors and energy absorption

of auxetic lattice cylindrical structures under axial crushing load", *Aerosp. Sci. Technol*., **98**, 105662. https://doi.org/10.1016/j.ast.2020.105662.

Gupta, A. and Pradyumna, S. (2022), "Nonlinear dynamic analysis of sandwich shell panels with auxetic honeycomb core and curvilinear fibre reinforced facesheets", *Eur. J. Mech. A Solids*, 95, 104640. https://doi.org/10.1016/j.euromechsol.2021.104640.

Han, D., Ren, X., Zhang, Y., Zhang, X.Y., Zhang, X.G., Luo, C. and Xie, Y.M. (2022), "Lightweight auxetic metamaterials: Design and characteristic study", *Compos. Struct*., **293**, 115706. https://doi.org/10.1016/j.compstruct.2022.115706.

Hoang, V.N.V. and Thanh, P.T. (2025), "Free vibration and nonlinear transient analysis of functionally graded graphene origami-enabled auxetic metamaterial cylindrical shells: Analytical and artificial neural network approaches", *Mech. Based Des. Struct. Mach.*, 1-44. https://doi.org/10.1080/15397734.2025.2145673.

Hu, Q., Zhang, X., Zhang, J., Lu, G. and Tse, K.M. (2024), "A review on energy absorption performance of auxetic composites with fillings", *Thin Wall. Struct*., 112348. https://doi.org/10.1016/j.tws.2024.112348.

Jiang, J.W., Kim, S.Y. and Park, H.S. (2016), "Auxetic nanomaterials: Recent progress and future development", *Appl. Phys. Rev*., **3**(4). https://doi.org/10.1063/3.0004445.

Karimiasl, M. and Alibeigloo, A. (2023), "Nonlinear aeroelastic analysis of sandwich composite cylindrical panel with auxetic core subjected to the thermal environment", *J. Vib. Control,* **29**(13-14), 3275-3297. https://doi.org/10.1177/10775463211012235.

Khorshidi, K., Savvafi, S. and Zobeid, S. (2025), "Investigation of free vibration in fluid-loaded cylindrical shells with a three-layer sandwich wall and an auxetic central layer", *Mech. Adv. Compos. Struct.,* **12**(1), 53-72. https://doi.org/10.1080/15712488.2025.2140070.

Kolken, H.M. and Zadpoor, A.A. (2017), "Auxetic mechanical metamaterials", *RSC Adv*., **7**(9), 5111-5129. https://doi.org/10.1039/C6RA23195B.

Lam, K.Y. and Loy, C.T. (1995), "Effects of boundary conditions on frequencies of a multi-layered cylindrical shell", *J. Sound Vib*., **188**(3), 363-384. https://doi.org/10.1006/jsvi.1995.0168.

Lee, Y.S. (2009), "Review on the cylindrical shell research", *Trans. Korean Soc. Mech. Eng. A*, **33**(1), 1-26. https://doi.org/10.3795/KSME-A.2009.33.1.1.

Li, B. and Fu, T. (2022), "Analysis of vibration characteristics of auxetic sandwich cylindrical shells resting on elastic foundation", *J. Sandw. Struct. Mater*., **24**(5), 1865-1882. https://doi.org/10.1177/1099636221996153.

Lim, T.C. (2015), *Auxetic Materials and Structures*, **33**, Springer Singapore, Singapore. https://doi.org/10.1007/978-981-10-1544-6.

Lvov, V.A., Senatov, F.S., Veveris, A.A., Skrybykina, V.A. and Díaz Lantada, A. (2022), "Auxetic metamaterials for biomedical devices: Current situation, main challenges, and research trends", *Materials*, **15**(4), 1439. https://doi.org/10.3390/ma15041439.

Ly, L.N., Duc, V.M., Trung, N.T., Phuong, N.T., Dong, D.T., Minh, T.Q., Tien, N.V. and Hung, V.T. (2021), "An analytical approach to the nonlinear buckling behavior of axially compressed auxetic-core cylindrical shells with carbon nanotube-reinforced coatings", *Proceedings of the Institution of Mechanical Engineers, Part L: Journal of Materials: Design and Applications*, **235**(10), 2254-2265. https://doi.org/10.1177/14644207211001737.

Mardling, P., Alderson, A., Jordan-Mahy, N. and Le Maitre, C.L. (2020), "The use of auxetic materials in tissue engineering", *Biomater. Sci*., **8**(8), 2074-2083. https://doi.org/10.1039/C9BM01221K.

Mir, M., Ali, M.N., Sami, J. and Ansari, U. (2014), "Review of mechanics and applications of auxetic structures", *Adv. Mater. Sci. Eng*., **2014**(1), 753496. https://doi.org/10.1155/2014/753496.

Mirfatah, S.M., Salehipour, H. and Civalek, Ö. (2024), "Geometrically nonlinear vibration of toroidal sandwich shells with auxetic honeycomb core under periodic/impulsive pressure", *Composite Struct*., **339**, 118166. https://doi.org/10.1016/j.compstruct.2024.118166.

Misseroni, D., Pratapa, P.P., Liu, K., Kresling, B., Chen, Y., Daraio, C. and Paulino, G.H. (2024), "Origami engineering", *Nat. Rev. Meth. Primers*, **4**(1), 40. https://doi.org/10.1038/s43586-023-00304-1.

Papadopoulou, A., Laucks, J. and Tibbits, S. (2017), "Auxetic materials in design and architecture", *Nat. Rev. Mater*., **2**(12), 1-3. https://doi.org/10.1038/natrevmats.2017.103.

Pasternak, H., Li, Z., Juozapaitis, A. and Daniūnas, A. (2022), "Ring stiffened cylindrical shell structures: State-of-the-art review", *Appl. Sci*., **12**(22), 11665. https://doi.org/10.3390/app122211665.

Pellicano, F. and Avramov, K.V. (2007), "Linear and nonlinear dynamics of a circular cylindrical shell connected to a rigid disk", *Commun. Nonlinear Sci. Numer. Simul*., **12**(4), 496-518. https://doi.org/10.1016/j.cnsns.2006.01.012.

Ren, X., Das, R., Tran, P., Ngo, T.D. and Xie, Y.M. (2018a), "Auxetic metamaterials and structures: A review", *Smart Mater. Struct*., **27**(2), 023001. https://doi.org/10.1088/1361-665X/aaa9f3.

Ren, X., Das, R., Tran, P., Ngo, T.D. and Xie, Y.M. (2018b), "Auxetic metamaterials and structures: A review", *Smart Mater. Struct*., **27**(2), 023001. https://doi.org/10.1088/1361-665X/aaa9f3.

Samadzadeh, M.H., Arefi, M. and Loghman, A. (2024), "Static bending analysis of pressurized cylindrical shell made of graphene origami auxetic metamaterials based on higher-order shear deformation theory", *Heliyon*, **10**(16). https://doi.org/10.1016/j.heliyon.2024.e12987.

Shen, H.S. (2012), "Nonlinear vibration of shear deformable FGM cylindrical shells surrounded by an elastic medium", *Compos. Struct*., **94**(3), 1144-1154. https://doi.org/10.1016/j.compstruct.2011.09.012.

Srinivas, S. (1974), *Analysis 0f Laminated, Composite, Circular Cylindrical Shells with General Boundary Conditions*, NASA-TR-R-412.

Wang, Y. and Wu, D. (2017), "Free vibration of functionally graded porous cylindrical shell using a sinusoidal shear deformation theory", *Aerosp. Sci. Technol*., **66**, 83-91. https://doi.org/10.1016/j.ast.2017.03.005.

Wang, Y.Q., Guo, X.H., Chang, H.H. and Li, H.Y. (2010), "Nonlinear dynamic response of rotating circular cylindrical shells with precession of vibrating shape—Part I: Numerical solution", *Int. J. Mech. Sci*., **52**(9), 1217-1224. https://doi.org/10.1016/j.ijmecsci.2010.06.013.

Wang, Y.Q., Ye, C. and Zu, J.W. (2019), "Nonlinear vibration of metal foam cylindrical shells reinforced with graphene platelets", *Aerosp. Sci. Technol*., **85**, 359-370. https://doi.org/10.1016/j.ast.2018.10.012.

Wang, Z., Luan, C., Liao, G., Liu, J., Yao, X. and Fu, J. (2020), "Progress in auxetic mechanical metamaterials: Structures, characteristics, manufacturing methods, and applications", *Adv. Eng. Mater*., **22**(10), 2000312. https://doi.org/10.1002/adem.202000312.

Xuebin, L. (2008), "Study on free vibration analysis of circular cylindrical shells using wave propagation", *J. Sound Vib*., 311(3-5), 667-682. https://doi.org/10.1016/j.jsv.2007.11.018.

Yang, N., Zou, Y. and Arefi, M. (2024), "Bending results of graphene origami reinforced doubly curved shell", *Defence*

Technol., **35**, 198-210. https://doi.org/10.1016/j.dt.2023.04.001.
Zhang, W., Hao, Y.X. and Yang, J. (2012), "Nonlinear dynamics of FGM circular cylindrical shell with clamped–clamped edges", *Compos. Struct*., **94**(3), 1075-1086. https://doi.org/10.1016/j.compstruct.2011.12.023.
Zhao, S., Zhang, Y., Zhang, Y., Yang, J. and Kitipornchai, S. (2021), "Graphene origami-enabled auxetic metallic metamaterials: An atomistic insight", *Int. J. Mech. Sci*., **212**, 106814. https://doi.org/10.1016/j.ijmecsci.2021.106814.
Zhao, S., Zhang, Y., Zhang, Y., Yang, J. and Kitipornchai, S. (2022), "Vibrational characteristics of functionally graded graphene origami-enabled auxetic metamaterial beams based on machine learning assisted models", *Aerosp. Sci. Technol*., **130**, 107906. https://doi.org/10.1016/j.ast.2022.107906.
Zhao, S., Zhang, Y., Zhang, Y., Zhang, W., Yang, J. and Kitipornchai, S. (2022), "Genetic programming-assisted micro-mechanical models of graphene origami-enabled metal meta-materials", *Acta Mater*., **228**, 117791. https://doi.org/10.1016/j.actamat.2022.117791.
Zippo, A., Barbieri, M., Iarriccio, G. and Pellicano, F. (2020), "Nonlinear vibrations of circular cylindrical shells with thermal effects: An experimental study", *Nonlinear Dyn*., **99**, 373-391. https://doi.org/10.1007/s11071-019-05130-7.

CC

Appendix

Appendix 1

$$L_{11}(u) = A_{11}\frac{\partial^2 u}{\partial x^2} + A_{66}\frac{\partial^2 u}{\partial t^2}$$

$$L_{12}(v) = \left(A_{12} + A_{66} - \frac{B_{12}+B_{66}}{R}\right)\frac{\partial^2 v}{\partial x \partial \theta}$$

$$L_{13}(w) = -\frac{A_{12}}{R}\frac{\partial w}{\partial x} - B_{11}\frac{\partial^3 w}{\partial x^3} - (B_{12}+2B_{66})\frac{\partial^3 w}{\partial x \partial \theta^2}$$

$$P_1(w) = A_{11}\frac{\partial w}{\partial x}\frac{\partial^2 w}{\partial x^2} + (A_{12}+A_{66})\frac{\partial w}{\partial \theta}\frac{\partial^2 w}{\partial x \partial \theta} + A_{66}\frac{\partial w}{\partial x}\frac{\partial^2 w}{\partial \theta^2}$$

$$L_{21}(u) = \left(A_{12} + A_{66} - \frac{B_{12}+B_{66}}{R}\right)\frac{\partial^2 u}{\partial x \partial \theta}$$

$$L_{22}(v) = \left(A_{66} - \frac{2B_{66}}{R} + \frac{D_{66}}{R^2}\right)\frac{\partial^2 v}{\partial x^2} + \left(A_{11} - \frac{2B_{11}}{R} + \frac{D_{11}}{R^2}\right)\frac{\partial^2 v}{\partial \theta^2}$$

$$L_{23}(w) = -\left(\frac{A_{11}}{R} - \frac{B_{11}}{R^2}\right)\frac{\partial w}{\partial \theta} - \left(B_{11} - \frac{D_{11}}{R}\right)\frac{\partial^3 w}{\partial \theta^3} + \left(B_{12} + 2B_{66} - \frac{D_{12}+2D_{66}}{R}\right)\frac{\partial^3 w}{\partial x^2 \partial \theta}$$

$$P_2(w) = \left(A_{66} - \frac{B_{66}}{R}\right)\frac{\partial^2 w}{\partial x^2}\frac{\partial w}{\partial \theta} + \left(A_{11} - \frac{B_{11}}{R}\right)\frac{\partial w}{\partial \theta}\frac{\partial^2 w}{\partial \theta^2} + \left(A_{12} + A_{66} - \frac{B_{12}+B_{66}}{R}\right)\frac{\partial w}{\partial x}\frac{\partial^2 w}{\partial x \partial \theta}$$

$$L_{31}(u) = \frac{A_{12}}{R}\frac{\partial u}{\partial x} + B_{11}\frac{\partial^3 u}{\partial x^3} + (B_{12}+2B_{66})\frac{\partial^3 u}{\partial x \partial \theta^2}$$

$$L_{32}(v) = \left(\frac{A_{11}}{R} - \frac{B_{11}}{R^2}\right)\frac{\partial v}{\partial \theta} + \left(B_{11} - \frac{D_{11}}{R}\right)\frac{\partial^3 v}{\partial \theta^3} + \left(B_{12} + 2B_{66} - \frac{D_{12}+2D_{66}}{R}\right)\frac{\partial^3 v}{\partial x^2 \partial \theta}$$

$$L_{33}(w) = -\frac{A_{11}}{R^2}w - 2\frac{B_{11}}{R^2}\frac{\partial^2 w}{\partial \theta^2} - D_{11}\left(\frac{\partial^2 w}{\partial x^4} + \frac{\partial^2 w}{\partial \theta^4}\right) - 2(D_{12}+2D_{66})\frac{\partial^2 w}{\partial x^2 \partial \theta^2}$$

$$P_3(w) = +2(A_{12}+2A_{66})\frac{\partial w}{\partial x}\frac{\partial w}{\partial \theta}\frac{\partial^2 w}{\partial x \partial \theta}$$

$$-\frac{w}{R}\left(A_{12}\frac{\partial^2 w}{\partial x^2} + A_{11}\frac{\partial^2 w}{\partial \theta^2}\right) + 2(B_{66}-B_{12})\frac{\partial^2 w}{\partial x^2}\frac{\partial^2 w}{\partial \theta^2}$$

$$+2(B_{12}-B_{66})\left(\frac{\partial^2 w}{\partial x \partial \theta}\right) - \frac{A_{12}}{2R}\left(\frac{\partial w}{\partial x}\right)^2 - \frac{A_{11}}{2R}\left(\frac{\partial w}{\partial \theta}\right)^2 + \frac{3A_{11}}{2}\left[\frac{\partial^2 w}{\partial x^2}\left(\frac{\partial w}{\partial x}\right)^2 + \frac{\partial^2 w}{\partial \theta^2}\left(\frac{\partial w}{\partial \theta}\right)^2\right] + \left(\frac{A_{12}}{2} + A_{66}\right)\left[\frac{\partial^2 w}{\partial \theta^2}\left(\frac{\partial w}{\partial x}\right)^2 + \frac{\partial^2 w}{\partial x^2}\left(\frac{\partial w}{\partial \theta}\right)^2\right]^2$$

$$R_3(v,w) = \left(A_{12} - \frac{B_{12}}{R}\right)\frac{\partial v}{\partial \theta}\frac{\partial^2 w}{\partial x^2} + 2\left(A_{66} - \frac{B_{66}}{R}\right)\frac{\partial v}{\partial x}\frac{\partial^2 w}{\partial x \partial \theta} + \left(A_{11} - \frac{B_{11}}{R}\right)\left(\frac{\partial v}{\partial \theta}\frac{\partial^2 w}{\partial \theta^2} + \frac{\partial^2 v}{\partial \theta^2}\frac{\partial w}{\partial \theta}\right) + \left(A_{66} - \frac{B_{66}}{R}\right)\frac{\partial^2 v}{\partial x^2}\frac{\partial w}{\partial \theta} + \left(A_{12} + A_{66} - \frac{B_{12}+B_{66}}{R}\right)\frac{\partial^2 v}{\partial x \partial u}\frac{\partial w}{\partial x}$$

Appendix 2

$$l_{11} = -A_{11}\frac{\pi^2 m^2}{L^2} - A_{66}\frac{n^2}{R^2}$$

$$l_{12} = l_{21} = \left(-A_{12} - A_{66} + \frac{B_{12}+B_{66}}{R}\right)\frac{\pi m n}{LR}$$

$$l_{13} = l_{31} = -A_{12}\frac{\pi m}{LR} + B_{11}\frac{\pi^3 m^3}{L^3} + (B_{12}+2B_{66})\frac{\pi m n^2}{LR^2}$$

$$l_{22} = \left(-A_{66} + \frac{2B_{66}}{R} - \frac{D_{66}}{R^2}\right)\frac{\pi^2 m^2}{L^2} + \left(-A_{11} + \frac{2B_{11}}{R} - \frac{D_{11}}{R^2}\right)\frac{n^2}{R^2}$$

$$l_{23} = l_{32} = \left(-\frac{A_{11}}{R} + \frac{B_{11}}{R^2}\right)\frac{n}{R} + \left(B_{11} - \frac{D_{11}}{R}\right)\frac{n^3}{R^3} + \left(B_{12} + 2B_{66} - \frac{D_{12}+2D_{66}}{R}\right)\frac{\pi^2 m^2 n}{L^2 R}$$

$$l_{33} = 2B_{12}\frac{\pi^2 m^2}{L^2 R} + 2B_{11}\frac{n^2}{R^3} - D_{11}\frac{\pi^4 m^4}{L^4} - D_{11}\frac{n^4}{R^4} - 2(D_{12}+2D_{66})\frac{\pi^2 m^2 n^2}{L^2 R^2} - \frac{A_{11}}{R^2} + \frac{ph\pi^2 m^2}{L^2}$$

$$n_1 = -32A_{11}\frac{\pi m^2}{9L^3 n} + 16(A_{12}-A_{66})\frac{n}{9\pi L R^2}$$

$$n_2 = \left(-A_{66} + A_{12} + \frac{B_{66}-B_{12}}{R}\right)\frac{16m}{9L^2 R} + \left(-A_{11} + \frac{B_{11}}{R}\right)\frac{32n^2}{9\pi^2 R^3 m}$$

$$n_3 = 16A_{12}\frac{m}{3L^2 R n} + 16A_{11}\frac{n}{3\pi^2 R^3 m} + 32(B_{66}-B_{12})\frac{mn}{3L^2 R^2}$$

$$n_4 = -9A_{11}\frac{\pi^4 m^4}{32L^4} - (A_{12}+2A_{66})\frac{\pi^2 m^2 n^2}{16L^2 R^2} - 9A_{11}\frac{n^4}{32R^4}$$

$$n_5 = 32A_{11}\frac{\pi m^2}{9L^3 n} + 32(A_{12}-A_{66})\frac{n}{9\pi L R^2}$$

$$n_6 = \left(A_{12} - A_{66} + \frac{B_{66}-B_{12}}{R}\right)\frac{32m}{9L^2 R} + \left(A_{11} - \frac{B_{11}}{R}\right)\frac{32n^2}{9\pi^2 R^3 m}$$